IEEE Access
Multidisciplinary ⋮ Rapid Review ⋮ Open Access Journal

Received 19 June 2024, accepted 24 July 2024, date of publication 31 July 2024, date of current version 9 August 2024.

Digital Object Identifier 10.1109/ACCESS.2024.3436078

RESEARCH ARTICLE

Radar Determination of Elevation of Two Nearby Targets Using Neural Network

PAVEL BEZOUŠEK AND SIMEON KARAMAZOV
Faculty of Electrical Engineering and Informatics, University of Pardubice, 532 10 Pardubice, Czech Republic
Corresponding author: Simeon Karamazov (simeon.karamazov@upce.cz)

ABSTRACT Monopulse methods have been successfully used in radar to determine the direction of arrival of a reflected signal, giving good results when a single isolated target is involved. However, when two nearby targets need to be detected and their angular position determined, this method fails. We show that it is possible to train and use a neural network to recognize two nearby targets. This neural network is then used to determine the angle of arrival of the reflected signal with sufficient accuracy, even when the distance of the targets is less than the beamwidth. We show the results on an eight-beam antenna model by measuring the elevation using an amplitude monopulse and neural network method. While using monopulse, we can reliably discriminate and determine the angular position of two targets only when their distance is larger than one beamwidth. The neural network method works reliably even for targets at distances much smaller.

INDEX TERMS Angle resolution, antenna beam, monopulse, neural network, radar.

I. INTRODUCTION

To determine the direction of arrival of a signal in a multibeam radar system, an amplitude or phase monopulse is usually used [1]. The advantage of monopulse methods is simple computation and good overall accuracy when only a single target is present in the vicinity of a given resolution cell. However, in the situation where multiple nearby targets are present in the same range cell, these methods fail.

Most of the properties of the two monopulse methods are comparable (especially accuracy). Phase monopulse has some advantages over amplitude monopulse, e.g., the monopulse characteristic is monotonic over a larger area around the monopulse axis, so that angle errors at the edges of the beams can be more easily eliminated. In a phase monopulse, the presence of two or more targets in a single cell can also be indicated using the imaginary component of the characteristic [2].

To resolve two targets using the monopulse method, their separation of one to two beamwidths is critical. Therefore, it is advisable to complement these methods with an additional method that allows the position of two targets to be determined with sufficient accuracy even at distances less than one beamwidth.

Many authors have therefore addressed the problem of detecting multiple targets and determining their precise angular position. The oldest method of indicating the presence of two or more targets in one cell is based on testing the nullity of the imaginary component of the phase monopulse characteristic [2]. However, the non-zero threshold of this method depends on the SNR (signal to noise ratio) and the DOA (direction of arrival) of the dominant target, which considerably complicates its applicability in practice. Later, other more robust methods have been developed, based on various assumptions about the target statistics [3], [4], [5], but usually at the cost of higher computational complexity or a complicated transmission scheme [6]. Recently, relatively fast algorithms have also been developed specifically for wideband tracking radars e.g., [6], [7]. However, the last projects were mainly concerned with extended targets with a large number of reflecting centers, such as jamming chaff or spawning munitions.

In this paper, we focus on elevation measurements for long-range (up to 450 km) 3D surveillance radars operating in track while scan (TWS) mode. The typical range resolution cell size for such radars is 200 m to 300 m. We will be mainly interested in the situation where a maximum of two aircrafts will be found in one range cell, each with one reflecting center (two point-reflectors). In the case of the presence of more than two targets in one resolution cell, our method evaluates only the presence of a target, without specifying its position in the cell. However, this situation is very unlikely for 3D surveillance radars, and is more typical for 2D radars with large vertical cell dimensions.

The associate editor coordinating the review of this manuscript and approving it for publication was Guolong Cui.

After processing in the signal processor we have the signals after pulse compression, Doppler filtering, and multilevel detection in several elevation beams. Thus, to determine the position of one and two targets in the same resolution cell, it is necessary to process the signals in individual elevation beams. For the purpose of amplitude and phase monopulse, sum and difference monopulse channels are created from adjacent beams and their characteristics are calculated.

However, improving the resolution of two or more nearby targets and refining their position can be achieved even without the use of monopulse by various adaptive methods, which are based on calculation of the so-called pseudospectrum of signals [8]. Pseudospectral (PS) methods are numerous, and they are usually divided into parametric and nonparametric types.

Non-parametric methods assume only that the signal is composed of periodic complex exponentials and noise. No other parameters need to be known. For antennas, this corresponds to receiving a signal from multiple point targets and noise. Typical nonparametric methods include the ASCE (Amplitude Spectra Capon Estimator) and APES (Amplitude Phase Estimator of Sinusoid) [9], [10].

Parametric methods need to specify some additional parameters, most often the number of targets. While there are a number of methods for estimating the number of targets, this can be difficult to solve in general. A group of methods, represented for example by the MUSIC (MUlti SIgnal Correlation analysis) algorithms [11], [12], solve the problem by decomposing the autocovariance matrix into eigenvectors, which then represent either signals or noise sources. The MUSIC algorithm has many variants, which differ in the transformations of the space of eigenvectors of the correlation matrix, or in the methods of solving the decomposition of the correlation matrix. There are also other algorithms based on this principle (e.g., ESPRIT, MODEM, RELAX [13]). The MUSIC algorithm is quite complicated and has been described in many publications.

Another group of high-resolution methods is based on an autoregressive (AR) model of the received signal. There are several modifications such as Burg's method [14], [15], the Yule - Walker method [16], and the covariance and modified covariance method [17]. Although these methods also provide better angle resolution, the accuracy of determining the angle of arrival of the signal tends to be lower.

It should be noted here however, that the beams produced by PS techniques depend on the particular distribution of targets and noise. This affects not only the shape but also the gain of the beam, so that the gain may be greater or even less than that of a standardly designed elevation beam. Calculations show that the differences between the SNR, achieved with beams designed by the ASCE method for a standard elevation beam, are in the range of about ±5 dB. This means that the required beam gain cannot be guaranteed and therefore this technology is generally not suitable for the detection of weak targets. Therefore, for the best detection, a standard beam with maximum gain (e.g., a summed monopulse beam) should be used. With sufficient SNR, one of the aforementioned pseudospectral methods can then be used to improve the angle resolution, if necessary.

In this paper, we show that the improvement in angle resolution can be achieved without loss of sensitivity and accuracy by processing the signal of all neighboring beams in which the targets appear. Although this method can be used to resolve targets and measure the angle of arrival of signals in any direction, in this paper we compare the calculations of only the elevation of two targets. The amplitude monopulse method and the artificial neural network method are used for this purpose. For the demonstration we chose a multibeam antenna with eight stacked beams in elevation, covering the elevation range −0.4° to 24°.

The antenna is a planar array for a new version of the long-range 3D S band radar ELDIS RL-3000, consisting of 47 horizontal end-fed slotted waveguide rows each with 107 slots [18]. Each row creates a beam of 1.25° beamwidth in azimuth. The vertical cosecant-shape transmitting beam is formed using only phase control of the rows. Their amplitude (power) is kept constant to optimize the efficiency of the high-power amplifiers of the transmitter. The vertical shapes of the receiving beams are determined in the digital beam forming network. The beams heading to the lowest elevations should detect the furthest radar targets and therefore they should have the highest gain and thus the narrowest beamwidth possible. Beams at higher elevations can show wider beamwidths due to a better height resolution at the shorter range and higher received signals from the nearer targets. The beams were designed using a Taylor/35 dB response. Nevertheless, in our computation we use only a Gaussian approximation.

II. MATHEMATICAL DESCRIPTION

A. SINGLE TARGET SIGNAL DETECTION

We assume M antenna beams, and a signal from one target with elevation $\boldsymbol{\Theta_1}$, amplitude $\boldsymbol{A_1}$ and phase $\boldsymbol{\varphi_1}$. Such a signal can be expressed in the mth beam as

$$s_m = A_1 \exp(\mathrm{j}\varphi_1)\, z(\Theta_{0m} - \Theta_1) + n_m, \quad m = 1, 2, \ldots, M, \tag{1}$$

where n_m is the noise voltage in the mth beam and the function $z(\theta_{0m} - \Theta_1)$ is the voltage characteristic of the mth beam, whose shape can be approximated by the waveform for a Gaussian beam expressed as

$$z(\Theta_{0m} - \Theta_1) = g_m \exp\left[-\frac{\ln(2)}{2}\left(\frac{\Theta_{0m} - \Theta_1}{\frac{\Theta_{3\mathrm{dB}m}}{2}}\right)^2\right] \quad \frac{\Theta_{0m} - \Theta_1}{\frac{\Theta_{3\mathrm{dB}m}}{2}} \leq 2, \tag{2}$$

and

$$z(\Theta_{0m} - \Theta_1) = 0 \quad \frac{\Theta_{0m} - \Theta_1}{\frac{\Theta_{3\mathrm{dB}m}}{2}} > 2, \tag{3}$$

where Θ_{0m} is the elevation of the mth beam axis, $\Theta_{3\mathrm{dB}m}$ is the beam width of the mth beam, and g_m is the ratio of the voltage gains of the mth beam to the voltage gain of the first beam. As we deal with an antenna with beams of different beamwidths (see Figure 1) the subscript m in $\Theta_{3\mathrm{dB}m}$ refers to the mth beam. Consequently, the gains of the individual beams are also different, which is expressed by different gains ratios g_m.

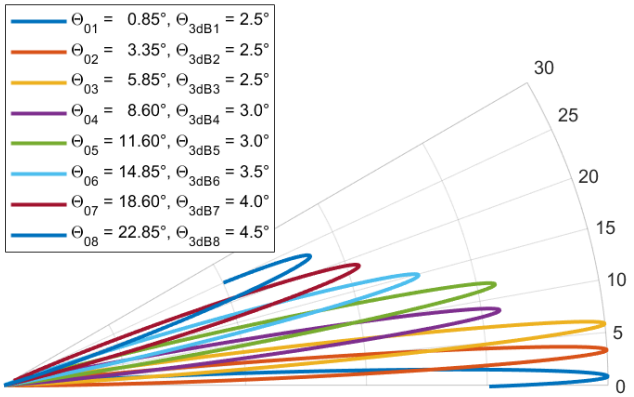

FIGURE 1. Illustration of the distribution of the eight elevation beams used to determine target elevations. The beam axis elevations and widths of each beam are given in the legend.

The set of functions describing the outputs of the M channels for a single target, equation (1), will be called here the elevation beams. Figure 1 shows a model example of the distribution of eight elevation beams. The beam axes elevations Θ_{0m} and the beamwidths $\Theta_{3\mathrm{dB}m}$ are shown in the legend of Figure 1. This beam layout model is derived from a real radar which we have used in all further calculations.

For further considerations, we assume that a single target can be simultaneously detected in at most three adjacent elevation beams, as shown in Figure 2.

B. AMPLITUDE MONOPULSE

For the purpose of amplitude monopulse, differential Δ_m and sum $\sum_m$ beams from adjacent elevation beams m a $m+1$ are created:

$$\begin{aligned} \Delta_m &= |s_{m+1}| - |s_m|\,, \\ \Sigma_m &= |s_{m+1}| + |s_m|\,, \\ & m = 1, 2, \ldots, M, \end{aligned} \tag{4}$$

and from them the characteristics of the monopulse β_m is calculated such that

$$\beta_m = \frac{\Delta_m}{\Sigma_m}. \tag{5}$$

The advantage of this procedure is that the characteristic (function) $\beta_m(\Theta)$ is dependent only on the elevation, since the amplitude A_1 and phase φ_1 are truncated in a fraction (5). The sum and difference beam pair (Σ_m, Δ_m) will be called the mth monopulse channel with the function $\beta_m(\Theta)$, for our model shown in Figure 3.

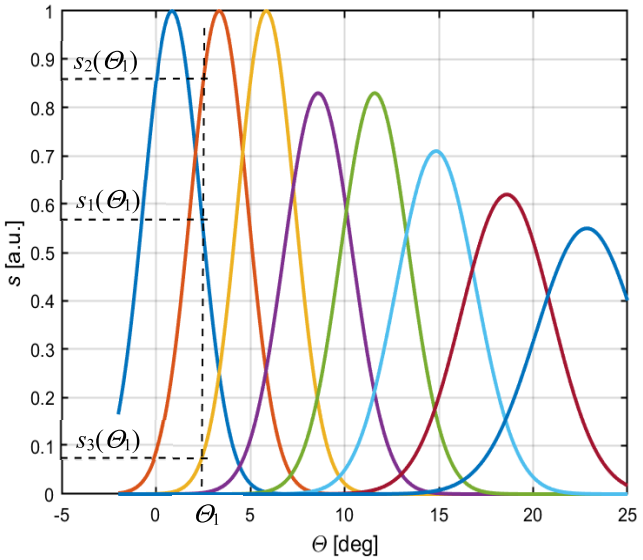

FIGURE 2. Example of a single target with elevation Θ_1 detected in the three adjacent elevation beams and producing three signals $s_1(\Theta_1)$, $s_2(\Theta_1)$, $s_3(\Theta_1)$.

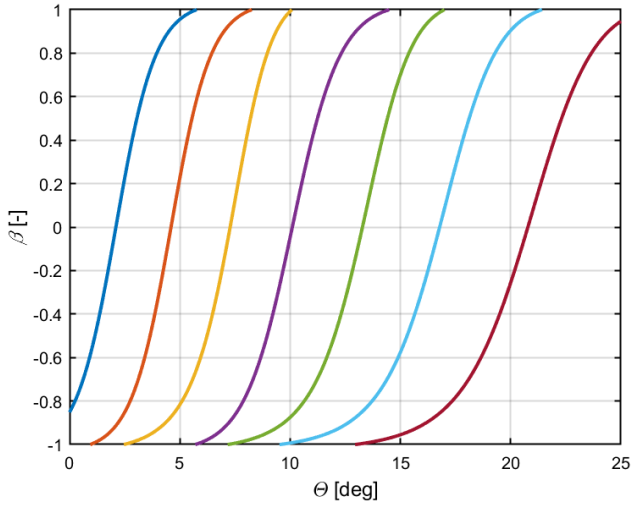

FIGURE 3. Dependencies of the β functions of seven monopulse channels $m = 1$ to $m = 7$ on the elevation of the targets. The different slopes of the curves correspond to different beams widths.

One target can be simultaneously detected in a maximum of three adjacent elevation beams, i.e., in two adjacent monopulse channels. That means we can have measurements of the functions $\beta_m(\Theta)$ from one or two monopulse channels for one target.

In the presence of a single target detected in three adjacent elevation beams, i.e., $m = k$, $k+1$ a $k+2$, the following relations are obtained

$$\beta_m = \frac{z(\Theta_{0m+1} - \Theta_1) + \eta_{m+1} - z(\Theta_{0m} - \Theta_1) - \eta_m}{z(\Theta_{0m+1} - \Theta_1) + \eta_{m+1} + z(\Theta_{0m} - \Theta_1) + \eta_m}, \tag{6}$$

where

$$\eta_m = \frac{n_m}{A_1}. \tag{7}$$

Noises η_m in all beams (n_m is the noise in the mth beam) are considered uncorrelated. Inverse functions to functions $\beta_m(\Theta_1)$ we denote by $\Theta_{m1}(\beta_{m1})$. We then compute the target elevation from measured values β_{m1}.

$$\Theta_1 = \frac{1}{2}\sum_{m=k}^{k+1}\Theta_{m1}(\beta_{m1}). \tag{8}$$

From this relationship, we can estimate the errors due to noise assuming a large SNR. We can expect that small and uncorrelated noise quantities η_m will cause small deviations $\delta\beta_m$ of the measured values β_m

$$\beta_m \cong \beta_{m0} + \delta\beta_m, \tag{9}$$

where

$$\beta_{m0} = \beta_m(\eta_m = 0, \eta_{m+1} = 0), \tag{10}$$

$$\delta\beta_m = \left(\frac{\partial\beta_m}{\partial\eta_m}\bigg|_{\eta_m=0,\eta_{m+1}=0}\right)\eta_m + \left(\frac{\partial\beta_m}{\partial\eta_{m+1}}\bigg|_{\eta_m=0,\eta_{m+1}=0}\right)\eta_{m+1}, \tag{11}$$

$$\frac{\partial\beta_m}{\partial\eta_m}\bigg|_{\eta_m=0,\eta_{m+1}=0} = -\frac{1+\beta_m}{z(\Theta_{0m+1}-\Theta_1)+z(\Theta_{0m}-\Theta_1)}, \tag{12}$$

$$\frac{\partial\beta_m}{\partial\eta_{m+1}}\bigg|_{\eta_m=0,\eta_{m+1}=0} = -\frac{\beta_m-1}{z(\Theta_{0m+1}-\Theta_1)+z(\Theta_{0m}-\Theta_1)}. \tag{13}$$

We will obtain

$$\delta\beta_m \cong \frac{(1-\beta_m).\eta_{m+1}-(1+\beta_m)\eta_m}{z(\Theta_{0m+1}-\Theta_1)+z(\Theta_{0m}-\Theta_1)}. \tag{14}$$

This creates an error $\delta\Theta_1$ of the calculated target elevation Θ_1

$$\delta\Theta_1 \cong \frac{1}{2}\sum_{m=k}^{k+1}\frac{\partial\Theta_{k1}(\beta_m)}{\partial\beta_m}\delta\beta_m \equiv \frac{1}{2}(a_k\eta_k + b_k\eta_{k+1} + c_k\eta_{k+2}), \tag{15}$$

where

$$a_k = -\frac{\partial\Theta_{k1}(\beta_k)}{\partial\beta_k}\frac{(1+\beta_k)}{z(\Theta_{0k+1}-\Theta_1)+z(\Theta_{0k}-\Theta_1)}, \tag{16}$$

$$b_k = \frac{\partial\Theta_{k1}(\beta_k)}{\partial\beta_k}\frac{(1-\beta_k)}{z(\Theta_{0k+1}-\Theta_1)+z(\Theta_{0k}-\Theta_1)} - \frac{\partial\Theta_{k+1,1}(\beta_{k+1})}{\partial\beta_{k+1}}\frac{(1+\beta_{k+1})}{z(\Theta_{0k+2}-\Theta_1)+z(\Theta_{0k+1}-\Theta_1)} \tag{17}$$

$$c_k = \frac{\partial\Theta_{k+1,1}(\beta_{k+1})}{\partial\beta_{k+1}}\frac{(1-\beta_{k+1})}{z(\Theta_{0k+2}-\Theta_1)+z(\Theta_{0k+1}-\Theta_1)}. \tag{18}$$

From here the variance $\sigma^2_{\Theta k}$ of the measured value Θ_1 in the kth monopulse channel can be calculated, assuming that the quantities $\eta_k, \eta_{k+1}, \eta_{k+2}$are uncorrelated and have zero mean.

$$\sigma^2_{\Theta k} = \frac{1}{4}\left(a_k^2\sigma^2_{\eta k} + b_k^2\sigma^2_{\eta k+1} + c_k^2\sigma^2_{\eta k+2}\right), \tag{19}$$

where $\sigma^2_{\eta k}$ is a variance of η_k. And, if they are the same,

$$\sigma^2_{\eta k} = \sigma^2_{\eta k+1} = \sigma^2_{\eta k+2} = \frac{1}{SNR}. \tag{20}$$

Then it gives

$$\sigma^2_{\Theta k} = \frac{1}{4}\left(\frac{a_k^2}{SNR} + \frac{b_k^2}{SNR} + \frac{c_k^2}{SNR}\right) = \frac{1}{4SNR}\left(a_k^2 + b_k^2 + c_k^2\right). \tag{21}$$

C. TWO NEARBY TARGETS

We will now assume that two targets are located in the same range resolution cell and in the same or nearby elevation cells. Targets are characterized by amplitudes A_1, A_2, phases φ_1, φ_2, and elevations Θ_1, Θ_2. In the case of two targets, relation (1) for the signals in each beam will be modified as follows

$$s_m = A_1\exp(\mathrm{j}\varphi_1)\,z(\Theta_{0m}-\Theta_1) + A_2\exp(\mathrm{j}\varphi_2)\,z(\Theta_{0m}-\Theta_2) + n_m. \tag{22}$$

With two targets, measurements from one or two monopulse channels can be obtained depending on target positions. The effect of the second target on the accuracy of the first target elevation measurement is negligible with large target separation. In this case, the targets can be determined independently. However, as the targets get closer in elevation, the situation will arise that outputs from three elevation beams will be available, but a signal of one beam will be composed of contributions of both targets. Then we can calculate the elevation of the two targets, but with a certain error, which will already include not only noise, but also the influence of the second target. If the targets approach at a distance smaller than the beam-width, the targets usually cannot be distinguished using the monopulse method.

It shows that the monopulse cannot determine the position of two nearby targets with sufficient accuracy when the targets are separated by less than two beamwidths. Therefore, we searched for a method that could determine the position of two targets, at least up to a distance less than one beamwidth.

For two targets, the amplitudes and phases of the individual targets can no longer be simply eliminated for the monopulse, as was done in fraction (5). Now to determine the elevations Θ_1, Θ_2 it will also be necessary to estimate the quantities $A_1, A_2, \varphi_1, \varphi_2$. Given the declared properties of the noise n_m (uncorrelated and normally distributed), the maximum likelihood (ML) condition will be one where the sum of the squares of the deviations of model (22) from the received signals s_m in each channel is minimal (least squares).

We therefore introduce the quantity Ψ

$$\Psi\left(A_1, A_2, \varphi_1, \varphi_2, \Theta_1, \Theta_2\right) = \sum_{i=1}^{M} \left| s_m - A_1 \exp\left(\mathrm{j}\varphi_1\right) z\left(\Theta_{0m} - \Theta_1\right) + A_2 \exp\left(\mathrm{j}\varphi_2\right) z\left(\Theta_{0m} - \Theta_2\right) \right|^2 \quad (23)$$

and we will look for values of $A_1, A_2, \varphi_1, \varphi_2, \Theta_1, \Theta_2$, minimizing the expression Ψ. This can be done in several ways. For example, we can start from the condition of zero of the first derivatives of the function Ψ with respect to all variables. However, we get a system of nonlinear equations that are difficult to solve, and the existence of a single solution is not even guaranteed. This greatly complicates the calculations. To solve this problem we have therefore used artificial neural network.

III. NEURAL NETWORK FOR TWO NEARBY TARGETS

To determine the elevations of the two targets according to equation (23), most methods would require calculating all the parameters of the targets, often in a very complicated manner. Therefore, we designed a neural network with inputs that correspond to the number of signals from the antenna beams and only two outputs for the two elevations of interest. Input signals depend on all parameters mentioned above $(A_1, A_2, \varphi_1, \varphi_2, \Theta_1, \Theta_2,)$. Figure 4 shows structure of the designed neural network.

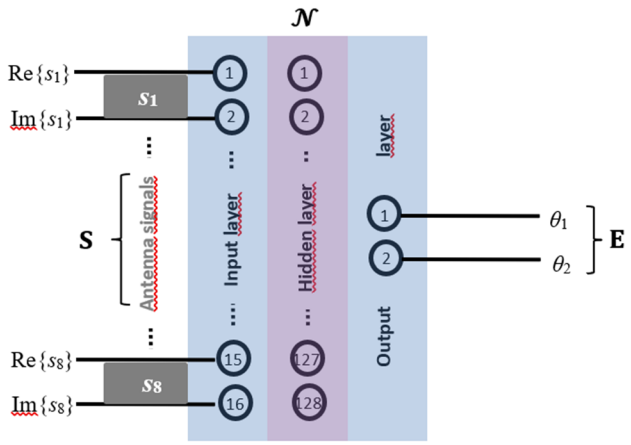

FIGURE 4. Structure of the neural network used to calculate the elevations of two nearby targets designed for eight (M=8) antenna beams.

If equation (22) for the signals s_m is formally rewritten in matrix form, we can consider the neural network $\mathcal{N}$ as a complex nonlinear matrix function for computing two nearby elevations. The following formal relation is

$$\mathbf{E} = \mathcal{N}\left(\mathbf{S}\right), \quad (24)$$

where the column vector $\mathbf{E}$ represents both elevations and the vector $\mathbf{S}$, is made up of complex signals from all beams.

$$\mathbf{E} = \begin{bmatrix} \Theta_1 \\ \Theta_2 \end{bmatrix}, \mathbf{S} = \begin{bmatrix} s_1 \\ \vdots \\ s_m \\ \vdots \\ s_M \end{bmatrix}. \quad (25)$$

It has been shown that a neural network with a single hidden layer can approximate any function [19], [20], [21].

Since the neural networks in the Matlab environment [22], [23] work with real values, it was necessary to use the signals $\mathbf{S}$ converted to their real and imaginary parts. This led to the fact that the complex signals from the M antenna beams (eight in our model) was represented at the input to the neural network $\mathcal{N}$ by $2M$ inputs. Thus, the input layer consisted of sixteen neurons in our neural network. As mentioned earlier, the output layer for the two elevations $\mathbf{E}$ of nearby targets was composed of two neurons.

The internal structure consisted of one or two layers of neurons. We tried several variants and with respect to accuracy and learning time-length, a network of one hidden layer with 128 neurons was found to be the most optimal variant. The scale and internal structure of the network can of course be extended, but we did not achieve any significant improvement in accuracy, and the learning time increases disproportionately with increasing network complexity.

The training set was constructed from 2.8×10^6 different combinations of variables $A_1, A_2, \varphi_1, \varphi_2, \Theta_1, \Theta_2$, and also noise n_m. Of this number of signal samples, 70% of them were randomly chosen for training, 15% for validation, and 15% for testing. A hyperbolic tangent sigmoid transfer function was used in the hidden layer and a linear transfer function in the output layer. The network was trained using the Levenberg-Marquardt algorithm, which proved to be the most efficient of the several algorithms tested.

Elevation Θ_1 was chosen in the range of 0° - 9,15° and elevation Θ_2 was chosen so that the difference was at most 2.5°. For testing purposes, we chose amplitude $A_1 = 1$ and phase $\varphi_1 = 0$, to limit the training set size and learning time. Amplitude A_2 changed in the range of 0 to 1 and the phase φ_2 in the range of 0 to 2π rad. All parameters thus chosen were included in the training set for SNR noise levels from 20 to 50 dB.

Figure 5 shows an example of the output from the above-mentioned neural network. In this figure, for illustration, 80 randomly chosen pairs of close elevations, whose difference was at most 2.5°, were calculated. The left plot (blue points) represents the elevation Θ_1, the right plot (red points) represents the elevation Θ_2. Parameters A_2, φ_2, and n_m varied randomly over the range of the training set, while the parameters $A_1 = 1, \varphi_1 = 0$ remained constant as was explained above. The horizontal axes of both plots show the selected elevations which, together with the other parameters mentioned above, enter the calculation of the signals s_m in

the individual beams (vector **S**) according to equation (22). The elevations calculated by the neural network are on the vertical axes. If the neural network results match the selected elevation, the point representing the result would lie on the black dashed line (quadrant axis). From the figure, it can be seen that the results agree well with the input values.

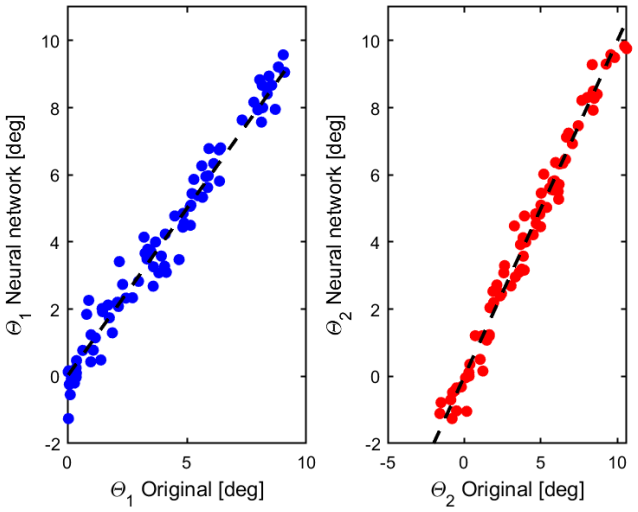

FIGURE 5. Elevations of two nearby targets computed by a neural network for 16 inputs (real and imaginary parts of signals from eight beams). Target parameter values were chosen randomly over the range of the training set for 80 pairs of nearby targets. The difference in target elevations was 2.5° at most.

For comparison, Figure 6 shows the calculation of elevations using the monopulse method with the same input values as were used to calculate the elevations shown in Figure 5. Comparing Fig. 5 and Fig. 6 we can see that the neural network gives much more accurate results for those target separations.

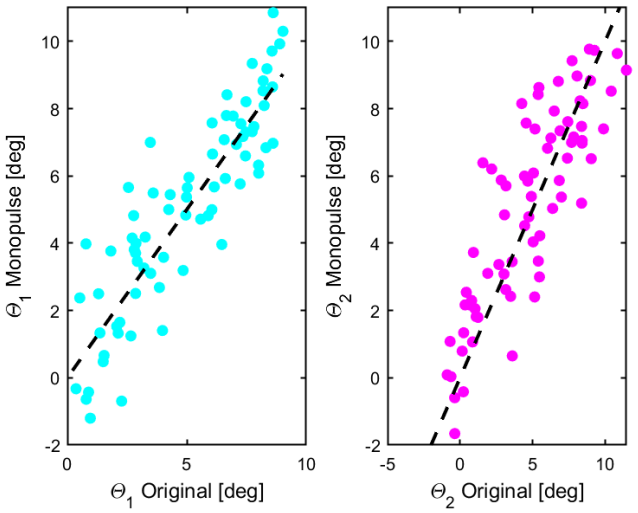

FIGURE 6. Elevations of two nearby targets calculated by the monopulse method. The parameters of both targets were chosen exactly as in the case of neural network calculations to allow easy comparison.

Figure 7 shows a comparison of the computation of elevations of two nearby targets using the monopulse method and the neural network. Parameters A_2, φ_2, and n_m varied randomly over the range of the training set, while the parameters $A_1 = 1, \varphi_1 = 0, \Delta\Theta = 2.5°$, SNR = 30 dB remained constant. The mean elevation $(\Theta_1 + \Theta_2)/2$ varied over the range of 0° to 3.5°. However, the difference $\Delta\Theta$ between elevations was kept constant and equal to the beamwidth Θ_{3dB1} of the first beam, i.e. $\Delta\Theta = \Theta_{3dB1} = 2.5°$.

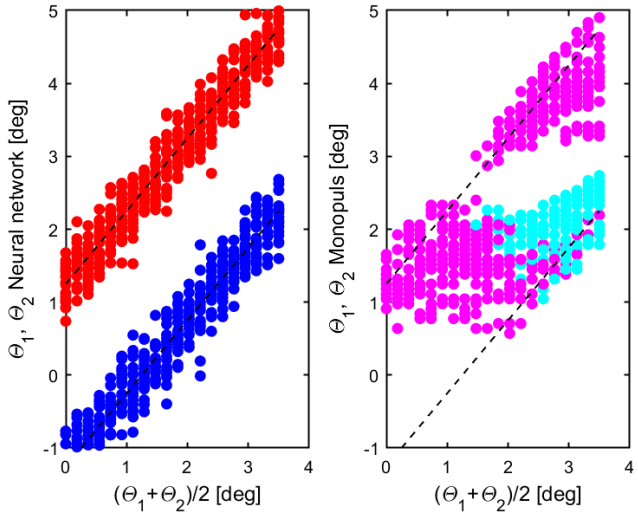

FIGURE 7. Elevations of 160 pairs of nearby targets computed by the neural network and the monopulse method. The values of the target parameters were chosen randomly over the range of the training set, and the difference of the elevations was constant $\Delta\Theta = 2.5° = \Theta_{3dB1,2,3}$.

The black dashed lines represent the actual elevations of the targets. The colored circles are the elevations calculated by the neural network method (left) and by the monopulse method (right) using exactly the same input parameters. We can see that while the calculation using neural networks still gives satisfactory results at a distance $\Delta\Theta = \Theta_{3dB1}$, in the case of the monpulse method the two targets overlap and therefore cannot be distinguished.

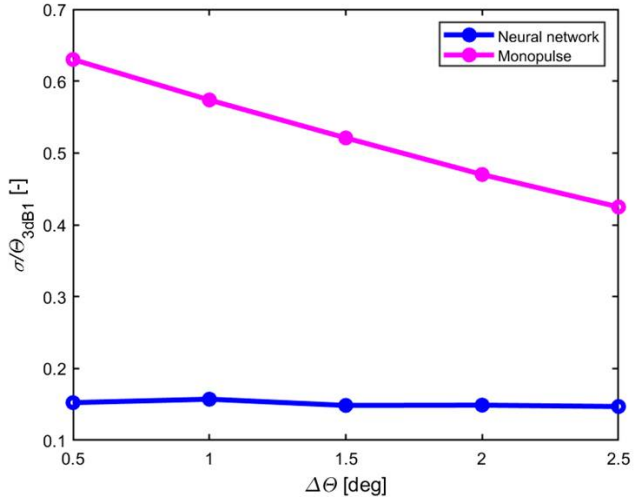

FIGURE 8. Comparison of the relative elevation errors calculated by the monopulse method and the neural network as a function of the elevation difference of the two targets.

Figure 8 also compares the methods of calculating the elevations of two nearby targets using monopulse or neural network - this time in terms of the errors of both methods. The sum of standard errors $\sigma_{\Theta k}$ i.e., the square roots of the variations (21) of the two targets relative to the beamwidth is presented as a function of the elevation difference $\Delta\Theta = \Theta_2 - \Theta_1$. This gives a better idea on how the errors of each method depend on the distance of the targets in elevation in antenna systems with beams of different beamwidths. The parameters of the first signal were chosen as before, $A_1 = 1, \varphi_1 = 0$, but SNR and the mean elevation were kept constant, SNR = 30 dB, $(\Theta_1 + \Theta_2)/2 = 2$. The other parameters $\eta A_2, \varphi_2, {}_k$ varied randomly. The errors were determined by averaging errors over all amplitudes A_2, phases φ_2, and noise η_k. It is evident that the errors of the monopulse method are significantly larger than those of the neural network method. Consistent with this theory is the fact that as the difference in elevations of the two nearby targets decreases, the errors of the monopulse method increase.

IV. CONCLUSION

By including target detections in all beams, the angle resolution and accuracy of the radar significantly improves compared to conventional procedures. This is demonstrated in a model with eight stacked beams in elevation. This approach is particularly suitable for 3D long range surveillance radar. A neural network was used to compute elevations from a large number of beams. Such a neural network can even be learned from data acquired during radar operation.

The results of the elevation calculations, obtained by applying the neural network, were compared with the results obtained by the amplitude monopulse method. It turns out that while the monopulse method is reliable only when the targets are more than one beamwidth apart, the neural network method allows accurate resolution of targets even below one beamwidth threshold. Once the targets are detected in standard beams, it will be possible to use the presented method at sufficient SNR to determine elevation, as a complement to the monopulse method.

REFERENCES

[1] M. A. Richards, J. A. Scheer, and W. A. Holm, *Principles of Modern Radar: Basic Principles*, document ISBN: 978-1-891121-52-4, 2010.

[2] P. L. Bogler, "Detecting the presence of target multiplicity," *IEEE Trans. Aerosp. Electron. Syst.*, vols. AES-22, no. 2, pp. 197–203, Mar. 1986.

[3] W. D. Blair and M. BrandtPearce, "Unresolved Rayleigh detection using monopulse measurements," *IEEE Trans. Aerosp. Electron. Syst.*, vol. 34, no. 1, pp. 543–552, Aug. 1998.

[4] U. R. O. Nickel, E. Chaumette, and P. Larzabal, "Statistical performance prediction of generalized monopulse estimation," *IEEE Trans. Aerosp. Electron. Syst.*, vol. 47, no. 1, pp. 381–404, Jan. 2011.

[5] J. D. Glass and W. D. Blair, "Detection of unresolved Rayleigh targets using adjacent bins," in *Proc. IEEE Aerosp. Conf.*, Mar. 2016, pp. 1–7, doi: 10.1109/AERO.2016.7500875.

[6] T. Tsai, Z. Liao, Z. Ding, Y. Zhao, and B. Tang, "Detection of unresolved targets for wideband monopulse radar," *Sensors*, vol. 19, no. 5, p. 1084, Mar. 2019.

[7] C. Tianyi, D. Bo, and H. Weibo, "Super-resolution parameter estimation of monopulse radar by wide-narrowband joint processing," *J. Syst. Eng. Electron.*, vol. 34, no. 5, pp. 1158–1170, Oct. 2023, doi: 10.23919/jsee.2023.000132.

[8] S. M. M. Tabatabaei Majd and B. Mohammadzadeh Asl, "Adaptive spectral Doppler estimation based on the modified amplitude spectrum capon," *IEEE Trans. Ultrason., Ferroelectr., Freq. Control*, vol. 68, no. 5, pp. 1664–1675, May 2021, doi: 10.1109/TUFFC.2020.3044774.

[9] A. Jakobsson and P. Stoica, "Combining Capon and APES for estimation of spectral lines," *Circuits, Syst., Signal Process.*, vol. 19, no. 2, pp. 159–169, Mar. 2000, doi: 10.1007/bf01212468.

[10] P. Stoica and A. Nehorai, "MUSIC, maximum likelihood, and cramer-rao bound," *IEEE Trans. Acoust., Speech, Signal Process.*, vol. 37, no. 5, pp. 720–741, May 1989.

[11] D. C. Rife and R. R. Boorstyn, "Multiple tone parameter estimation from discrete-time observations," *Bell Syst. Tech. J.*, vol. 55, no. 9, pp. 1389–1410, Nov. 1976.

[12] S. M. Kay, *Modern Spectral Estimation*. Upper Saddle River, NJ, USA: Prentice-Hall, 1988, ch. 1.

[13] A. L. Swindlehurst, B. Ottersten, R. Roy, and T. Kailath, "Multiple invariance ESPRIT," *IEEE Trans. Signal Process.*, vol. 40, no. 4, pp. 867–881, Apr. 1992.

[14] S. de Waele and P. M. T. Broersen, "The Burg algorithm for segments," *IEEE Trans. Signal Process.*, vol. 48, no. 10, pp. 2876–2880, Nov. 2000.

[15] K. Kazlauskas, "The Burg algorithm with extrapolation for improving the frequency estimation," *Informatica*, vol. 22, no. 2, pp. 177–188, Jan. 2011.

[16] P. Stoica, B. Friedlander, and T. Söderström, "A high-order Yule-Walker method for estimation of the AR parameters of an ARMA model," *Syst. Control Lett.*, vol. 11, no. 2, pp. 99–105, Aug. 1988.

[17] S. L. Marple, "A fast computational algorithm for the modified covariance method of linear prediction," *Digit. Signal Process.*, vol. 1, no. 3, pp. 124–133, Jul. 1991.

[18] *RL-3000 3D Long Range Air Surveillance Radar*, ELDIS Pardubice, s.r.o, 2024.

[19] K. Hornik, M. Stinchcombe, and H. White, "Multilayer feedforward networks are universal approximators," *Neural Netw.*, vol. 2, no. 5, pp. 359–366, Jan. 1989.

[20] H. W. Lin, M. Tegmark, and D. Rolnick, "Why does deep and cheap learning work so well?" *J. Stat. Phys.*, vol. 168, no. 6, pp. 1223–1247, Jul. 2017, doi: 10.1007/s10955-017-1836-5.

[21] I. J. Goodfellow, Y. Bengio, and A. Courville, *Deep Learning*. Cambridge, MA, USA: MIT Press, 2016.

[22] H. Demuth, M. Belae, and M. Hagan, *Neural Network Toolbox 6 User's Guide*. Natick, MA, USA: The MathWorks, 2008.

[23] D. Hanselman and B. Littelfield, *Mastering MATLAB 7*. Upper Saddle River, NJ, USA: Prentice-Hall, 2005.

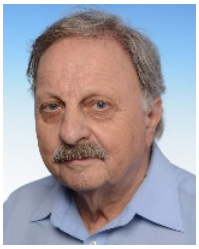

PAVEL BEZOUŠEK was born in Ostrava, Czechoslovakia, in 1943. He received the M.S. and Ph.D. degrees from Czech Technical University, Prague, in 1966 and 1980, respectively. He worked at the Radio Research Institute of Tesla Pardubice, from 1966 to 1994, where he was engaged in microwave circuit and system design. Since then, he has been with the University of Pardubice, where he is currently a Full Professor of radar system design with the Faculty of Electrical Engineering and Informatics.

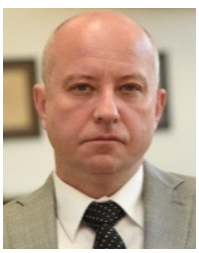

SIMEON KARAMAZOV was born in Pardubice, Czechoslovakia, in 1963. He received the Engineer's degree from Czech Technical University, Prague, in 1987, and the Ph.D. degree in solid-state physics and semiconductors from the University of Pardubice, in 1994. Since 1991, he has been working with the University of Pardubice, where he is currently a Full Professor with the Department of Mathematics and Physics, Faculty of Electrical Engineering and Informatics.